

Mitochondrial protection restores renal function in swine atherosclerotic renovascular disease

Alfonso Eirin¹, Behzad Ebrahimi¹, Xin Zhang¹, Xiang-Yang Zhu¹, John R. Woollard¹, Quan He², Stephen C. Textor¹, Amir Lerman³, and Lilach O. Lerman^{1,3*}

¹Division of Nephrology and Hypertension, Mayo Clinic, 200 First Street SW, Rochester, MN 55905, USA; ²Diabetes and Obesity Research Center, Sanford-Burnham Medical Research Institute, Orlando, FL, USA; and ³Division of Cardiovascular Diseases, Mayo Clinic, Rochester, MN, USA

Received 18 April 2014; revised 16 May 2014; accepted 20 May 2014; online publish-ahead-of-print 19 June 2014

Time for primary review: 14 days

Aims

The mechanisms responsible for renal injury in atherosclerotic renovascular disease (ARVD) are incompletely understood, and few therapeutic options are available to reverse it. We hypothesized that chronic renal damage involves mitochondrial injury, and that mitochondrial protection would reduce renal fibrosis and dysfunction in ARVD pigs.

Methods and results

Domestic pigs were studied after 10 weeks of ARVD or sham, treated for the last 4 weeks with daily subcutaneous injections (5 days/week) of vehicle or Bendavia (0.1 mg/kg), a tetrapeptide that preserves cardiolipin content in the mitochondrial inner membrane. Single-kidney haemodynamics and function were studied using fast-computer tomography, oxygenation using blood oxygen level-dependent magnetic resonance imaging, microvascular architecture, oxidative stress, and fibrosis *ex vivo*. Cardiolipin content was assessed using mass spectrometry and staining. Renal endothelial function was studied *in vivo* and *ex vivo*. In addition, swine renal artery endothelial cells incubated with *tert*-butyl hydroperoxide were also treated with Bendavia. Stenotic-kidney renal blood flow (RBF) and glomerular filtration rate (GFR) decreased in ARVD + Vehicle compared with normal (318.8 ± 61.0 vs. 553.8 ± 82.8 mL/min and 48.0 ± 4.0 vs. 84.0 ± 3.8 mL/min, respectively) associated with loss of cardiolipin, intra-renal microvascular rarefaction, and hypoxia. Bendavia restored cardiolipin content in ARVD and improved vascular density, oxygenation, RBF (535.1 ± 24.9 mL/min), and GFR (86.6 ± 11.2 mL/min). Oxidative stress and fibrosis were ameliorated, and renovascular endothelial function normalized both *in vivo* and *in vitro*.

Conclusion

Preservation of mitochondrial cardiolipin attenuated swine stenotic-kidney microvascular loss and injury, and improved renal oxygenation, haemodynamics, and function. These observations implicate mitochondrial damage in renal deterioration in chronic experimental ARVD, and position the mitochondria as a central therapeutic target.

Keywords

Hypertension • Renal • Atherosclerosis • Mitochondria

1. Introduction

Atherosclerotic renovascular disease (ARVD), a frequent cause of secondary hypertension in elderly individuals, conveys a significant risk for cardiovascular disease, as well as progression to chronic renal failure. Importantly, patients with ARVD exhibit considerable cardiovascular mortality, warranting the development of therapeutic interventions capable of protecting the kidney in this population.¹ The mechanisms responsible for irreversible kidney damage distal to a stenosis have not been fully elucidated, but seem to continue relentlessly even upon removal of the instigating injury. Hence, the negative clinical trials that show little benefit of revascularization alone in a growing population of

patients with ARVD create a cohort of patients with few therapeutic options to arrest kidney injury.²

Mitochondria produce 90% of cellular energy, sense levels of oxygen in the blood, and modulate the vasodilatory response mediated by endothelial nitric oxide.³ Moreover, increased mitochondrial production of intracellular reactive oxygen species (ROS) leads to vasoconstriction, compromising the renal microvasculature.⁴ Cardiolipin is a bisphosphatidyl glycerol lipid exclusively distributed in the inner mitochondrial membrane that regulates multiple mitochondrial activities, including electron transport chain (ETC) assembly and function, ATP biosynthesis, and apoptosis.^{5–7} Peroxidation and consequent loss of cardiolipin in ischaemia destabilizes the ETC, and triggers mitochondrial ROS

* Corresponding author. Tel: +1 507 266 9376; fax: +1 507 266 9316, Email: lerman.lilach@mayo.edu

production,⁸ opening of the mitochondrial permeability transition pore (mPTP), and release of cytochrome-c, thereby instigating apoptosis and oxidative damage.^{9,10} Thus, treatment strategies aimed to stabilize cardiolipin and protect mitochondria might attenuate progression to microvascular damage and dysfunction in the post-stenotic kidney.

Bendavia is a novel tetrapeptide that selectively and transiently concentrates in the inner mitochondrial membrane, where it binds to and stabilizes cardiolipin, facilitating efficient electron transport and preventing apoptosis.¹¹ Experimental studies have shown that Bendavia attenuates apoptosis and reperfusion injury associated with cardiovascular insults, and improves cardiac function and performance in several chronic models of heart failure.^{12–14} Furthermore, this strategy decreased renal fibrosis and oxidative stress in rats with unilateral ureteral obstruction¹⁵ and in mice with acute ischaemia–reperfusion injury,¹⁶ suggesting an important potential in ameliorating kidney injury in rodents.

We have recently shown that mitochondrial protection during revascularization by adjunct infusion of Bendavia preserved renal haemodynamics and function, and attenuated tissue injury in a swine model of ARVD, possibly by decreasing acute ischaemia–reperfusion injury.¹⁷ However, whether mitochondrial dysfunction contributes to chronic renal remodelling and dysfunction in ARVD remains to be elucidated. This study tested the hypothesis that cardiolipin stabilization and protecting mitochondrial function would reduce stenotic-kidney fibrosis and improve renal and vascular function in chronic non-revascularized experimental ARVD.

2. Methods

Twenty-eight female domestic pigs were studied after 16 weeks of observation (see Supplementary material online, *Figure S1*) after approval of the Mayo Clinic Institutional Animal Care and Use Committee.

At baseline, pigs were randomized in two groups of ARVD and normal controls ($n = 14$ each). While normal pigs were fed regular pig chow, ARVD pigs started a high cholesterol diet (see Supplementary material online, *Table S1*) in order to simulate the clinical situation in which diffuse early atherosclerosis precedes the stenosis.

Six weeks later, pigs were anaesthetized with 0.25 g of intramuscular tiletamine hydrochloride/zolazepam hydrochloride and 0.5 g of xylazine, and anaesthesia was maintained with intravenous ketamine (0.2 mg/kg/min) and xylazine (0.03 mg/kg/min). Renal artery stenosis was induced in ARVD pigs by placing a local-irritant coil in the main right renal artery, which leads to its gradual narrowing, as previously described.¹⁷ Normal pigs underwent a sham procedure.

Six weeks later, animals were similarly anaesthetized and the degree of stenosis determined by angiography (see Supplementary material online, *Figure S2*). A sham procedure was performed in all pigs. In addition, seven ARVD and seven normal pigs started treatment with chronic subcutaneous injection of Bendavia (MTP-131, SS-31, Stealth Peptides, Newton Centre, MA, USA), 0.1 mg/kg in 1 mL of phosphate-buffered saline (PBS) once daily 5 days/week. A PBS vehicle was injected in the remaining seven ARVD and seven normal pigs.

Four weeks later, the pigs were again similarly anaesthetized. The degree of stenosis was determined by angiography, and both systemic and renal venous blood samples collected for plasma renin activity (PRA), serum creatinine (both DiaSorin, Stillwater, MN, USA), and isoprostanes (enzyme immunoassay) measurements. Renal haemodynamics and function in each kidney were assessed using multi-detector computer tomography (MDCT), and renal oxygenation by blood oxygen level-dependent magnetic resonance imaging (BOLD-MRI).

After completion of all *in vivo* studies and 30–60 min after the last dose of Bendavia, pigs were euthanized with a lethal intravenous dose of sodium pentobarbital (100 mg/kg). The kidneys were dissected, and sections frozen in liquid nitrogen (and maintained at -80°C), prepared for micro-computer tomography (CT), or preserved in formalin for *in vitro* studies. Distal branches of the stenotic renal artery were dissected and placed in control solution for *in vitro* endothelial function studies.

2.1 *In vivo* studies

After 4 weeks of treatment, BOLD-MRI was performed at 3 T to measure the medullary and cortical relaxivity index $R2^*$.

One to two days later, stenotic-kidney cortical and medullary perfusions, renal blood flow (RBF), and glomerular filtration rate (GFR) were assessed using MDCT, which provide reliable and reproducible single-kidney measurements.¹⁸ Baseline measurements were repeated after 15 min towards the end of a 10-min suprarenal intra-aortic infusion of acetylcholine (Ach, 5 $\mu\text{g}/\text{kg}/\text{min}$) to test endothelium-dependent microvascular reactivity.

2.2 *In vitro* studies

2.2.1 Mitochondrial remodelling

Cardiolipin content was assessed by both mass spectrometry and staining, as well as mRNA expression of the cardiolipin regulators tafazzin (Taz)-1 and acyl-CoA:lysocardiolipin acyltransferase (ALCAT)-1.

2.2.2 Kidney injury mechanisms

Apoptosis was evaluated in stenotic-kidney sections by the terminal deoxynucleotidyl transferase-mediated dUTP nick end labelling (TUNEL) and activated caspase-3 staining, as well as renal protein expression of B-cell lymphoma-extra large (Bcl-xl) and Bcl2-associated X protein (Bax).

Renal redox status was evaluated by the *in situ* production of superoxide anion, detected by fluorescence microscopy using dihydroethidium (DHE), and by the expression of the radical-forming enzyme nicotinamide adenine dinucleotide phosphate hydrogen (NAD(P)H)-oxidase subunits p47 and p67.¹⁹

Tubular injury was scored (0–5) in renal tissue sections as described.¹⁷

Trichrome and collagen IV staining were semi-automatically quantified. Glomerular score was also quantified.²⁰ Renal expression of plasminogen activator inhibitor (PAI)-1, tissue inhibitor of metalloproteinase (TIMP)-1, and transforming growth factor (TGF)- β was determined by western blot.²¹

2.2.3 Microvascular architecture

Microvascular architecture was assessed using a micro-CT scanner. The spatial density, size, and tortuosity of microvessels in the inner, middle, and outer thirds of the renal cortex were calculated using AnalyzeTM. In addition, renal expression of vascular endothelial growth factor (VEGF) and angiotensin-1 was measured by western blot.¹⁷

2.2.4 Vascular endothelial function *ex vivo*

Dissected stenotic-kidney renal artery sections ($n = 8/\text{pig}$, 7 pigs/group) were progressively contracted with endothelin-1 (10^{-7} M) and increasing concentrations of Ach (10^{-9} – 10^{-4} M) were administered to evaluate endothelium-dependent relaxation, or endothelium-independent vasodilation with sodium nitroprusside (SNP, 10^{-9} – 10^{-4} M). Cardiolipin staining, apoptosis (TUNEL), production of superoxide anion (DHE), and endothelial nitric oxide synthase (eNOS) expression were assessed in these sections.

2.2.5 Endothelial cell studies

In vitro experiments were performed in primary cultures of swine renal artery endothelial cells (RAECs). RAECs were isolated from a normal animal, passaged several times, and used for different experiments at different times. First, cells were characterized by the expression of the endothelial markers CD31 and Von Willebrand factor (see Supplementary material online, *Figure S3*) and then RAECs were cultured and maintained at 37°C in endothelial culture media. Then, RAECs were divided into four groups

(six wells per group), which were grown in 24-well plates untreated or treated with either Bendavia 1 nM, tert-butyl hydroperoxide (tBHP) 30 μ M that causes lipid peroxidation and mitochondrial dysfunction,^{11,22} or tBHP + Bendavia for 6 h. Expression of caspase-3, nitrotyrosine, and phosphorylated eNOS was measured by western blot (six wells per group).

In addition, a different batch of RAECs from a similar passage were grown in staining chamber slides, untreated or treated with either Bendavia, tBHP, or tBHP + Bendavia at the same concentration and incubation time. These cells were subsequently stained for cardiolipin, caspase-3, DHE, and eNOS. The viability of RAEC was studied by trypan blue staining.

2.3 Statistical methods

Statistical analysis utilized the JMP software package. Results were expressed as mean \pm standard deviation. All studies included seven pigs/group, except for immunoblots ($n = 6$ pigs/group). Comparisons among and between the groups were performed by parametric (ANOVA and unpaired Student's *t*-test) and non-parametric (Wilcoxon and Kruskal–Wallis) tests when appropriate. A *P*-value of ≤ 0.05 was considered statistically significant.

For detailed Methods, see Supplementary material online.

3. Results

All ARVD animals achieved significant degrees of stenosis and renovascular hypertension (Table 1, all $P \leq 0.05$ vs. normal). Serum creatinine was higher in ARVD + Vehicle compared with normal, but improved in Bendavia-treated pigs. Systemic isoprostane levels remained elevated in both ARVD groups. Total, high-density lipoprotein, and low-density lipoprotein cholesterol levels were elevated in both ARVD + Vehicle and ARVD + Bendavia compared with normal. Stenotic-kidney volume, perfusion, RBF, and GFR were reduced in ARVD + Vehicle, but restored to normal levels in ARVD + Bendavia pigs (Table 1). Furthermore, RBF and GFR responses to Ach were both attenuated in ARVD + Vehicle compared with normal ($P = 0.034$ and 0.002 , respectively, vs. normal),

but not in ARVD + Bendavia ($P = 0.22$ and 0.13 , respectively, vs. normal). Cortical and medullary $R2^*$ values were elevated in ARVD + Vehicle compared with normal ($P = 0.014$ and 0.007 , respectively), suggesting hypoxia, which was normalized in Bendavia-treated ARVD (Figure 1).

3.1 Mitochondrial remodelling

Renal total cardiolipin content was decreased in ARVD + Vehicle but restored to normal levels in ARVD + Bendavia (Figure 2A) as were cardiolipin expression and staining intensity (Figure 2B). The most prominent molecular species affected were the tetra-linoleoyl (C18:2) followed by tetra-oleoyl (C18:1) cardiolipin, both normalized in ARVD + Bendavia (see Supplementary material online, Table S2 and Figure S4). Expression of taz-1 mRNA did not differ among the groups, whereas ALCAT-1 was down-regulated in ARVD + Bendavia animals (Figure 2C, $P = 0.003$ vs. normal, $P = 0.006$ vs. ARVD + Vehicle).

3.2 Kidney injury mechanisms

The numbers of cells positive for TUNEL and caspase-3 were elevated in ARVD + Vehicle compared with normal, yet normalized in ARVD + Bendavia (Figure 2D). Renal expression of Bax was similarly elevated in all ARVD pigs compared with normal, but Bendavia up-regulated the expression of Bcl-xl in ARVD (Figure 2E), and thus normalized Bax/Bcl-xl ratio in ARVD + Bendavia pigs ($P = 0.79$ vs. Normal + Vehicle).

In situ production of superoxide anion that increased in the post-stenotic ARVD kidney was normalized in ARVD + Bendavia (Figure 3A). Renal p47 (but not p67) expression was also restored in ARVD + Bendavia (Figure 3B).

Tubular injury score was elevated in both ARVD groups, yet improved in ARVD + Bendavia (Figure 3C). Immunostaining of collagen IV was elevated in ARVD, but normalized in ARVD + Bendavia (Figure 3D), and both tubulointerstitial fibrosis and glomerular score improved

Table 1 Systemic characteristics, single-kidney haemodynamics, and function in study groups ($n = 7$ each) at 16 weeks

Parameter	Normal + Vehicle	NORMAL + Bendavia	ARVD + Vehicle	ARVD + Bendavia
Degree of stenosis (%)	0	0	89.8 \pm 5.2*	81.0 \pm 5.3*
Body weight (kg)	51.8 \pm 3.6	49.8 \pm 8.2	55.8 \pm 1.8	58.4 \pm 6.3
Mean blood pressure (mmHg)	82.2 \pm 41.6	84.4 \pm 23.7	122.7 \pm 8.9*	123.4 \pm 4.4*
Serum creatinine (mg/dL)	1.5 \pm 0.2	1.5 \pm 0.1	1.9 \pm 0.3*	1.7 \pm 0.3
Plasma renin activity (ng/mL/h)	0.16 \pm 0.08	0.13 \pm 0.11	0.16 \pm 0.11	0.19 \pm 0.08
Isoprostane (pg/mL)	120.4 \pm 12.3	112.7 \pm 14.9	201.2 \pm 40.6*	194.4 \pm 30.2*
Total cholesterol (mg/dL)	92.5 \pm 20.6	84.8 \pm 6.9	487.3 \pm 53.9*	563.0 \pm 97.0*
HDL cholesterol (mg/dL)	42.8 \pm 16.3	48.2 \pm 6.4	180.4 \pm 58.6*	196.8 \pm 47.1*
LDL cholesterol (mg/dL)	48.2 \pm 11.0	34.8 \pm 6.3	305.2 \pm 77.9*	384.5 \pm 142.1*
Triglycerides (mg/dL)	8.0 \pm 2.4	9.2 \pm 3.8	9.6 \pm 8.5	5.8 \pm 2.8
Renal volume (cm ³)	102.9 \pm 4.0	96.1 \pm 6.3	66.4 \pm 6.3*†	104.9 \pm 3.3
Cortical perfusion (mL/min/cm ³)	4.5 \pm 0.5	4.0 \pm 0.3	3.1 \pm 0.2*†	4.4 \pm 0.2
Medullary perfusion (mL/min/cm ³)	3.0 \pm 0.3	2.5 \pm 0.6	1.3 \pm 0.3*†	2.9 \pm 0.4
RBF (mL/min)	553.8 \pm 82.8	589.7 \pm 71.8	318.8 \pm 61.0*†	535.1 \pm 24.9
GFR (mL/min)	84.0 \pm 3.8	75.8 \pm 6.8	48.0 \pm 4.0*†	86.6 \pm 11.2
Δ RBF acetylcholine (mL/min)	178.4 \pm 63.2	184.5 \pm 60.7	33.1 \pm 11.2*†	92.0 \pm 14.0
Δ GFR acetylcholine (mL/min)	20.7 \pm 2.3	17.1 \pm 2.2	5.4 \pm 2.6*†	13.7 \pm 3.5

ARVD, atherosclerotic renovascular disease; HDL, high-density lipoprotein; LDL, low-density lipoprotein; RBF, renal blood flow; GFR, glomerular filtration rate.

* $P \leq 0.05$ vs. Normal + Vehicle.

† $P \leq 0.05$ vs. ARVD + Bendavia.

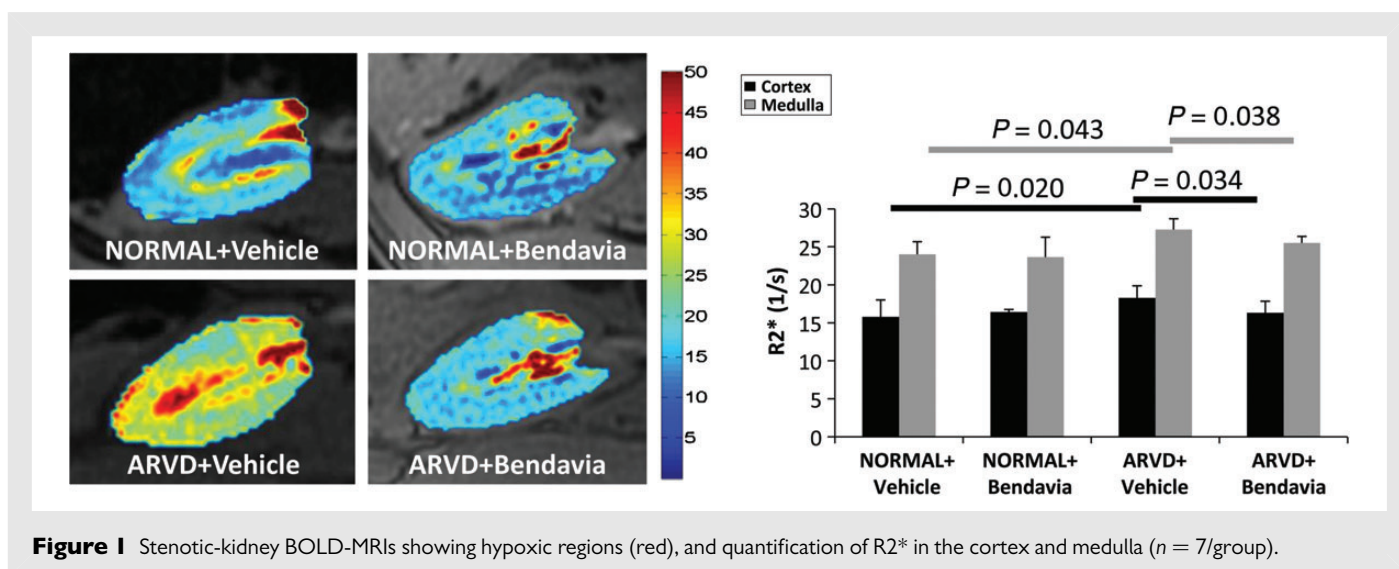


Figure 1 Stenotic-kidney BOLD-MRIs showing hypoxic regions (red), and quantification of $R2^*$ in the cortex and medulla ($n = 7/\text{group}$).

(Figure 4A). TGF- β remained up-regulated, but renal expression of PAI-1 and TIMP-1 was normalized in ARVD + Bendavia (Figure 4B).

PRA was similar among the groups, as typical to chronic untreated ARVD.²³

3.3 Microvascular remodelling

The spatial density of small (0.02 mm) microvessels in the inner cortex was similarly low in ARVD + Vehicle and ARVD + Bendavia animals. However, the number of small outer cortical microvessels slightly improved in Bendavia-treated pigs (Figure 5A) and microvascular tortuosity was normalized (Figure 5B). Renal expression of VEGF was blunted in ARVD, but markedly up-regulated by Bendavia, as was the expression of angiopoietin-1 (Figure 5C).

3.4 Vascular endothelial function ex vivo

The vasorelaxation response to Ach in renal vessels of ARVD + Vehicle pigs was attenuated, but normalized in ARVD + Bendavia (Figure 6A), whereas the response to SNP was unaltered.

Cardiolipin expression was decreased in ARVD renal artery rings, but improved in ARVD + Bendavia (Figure 6B, $P = 0.001$ vs. ARVD + Vehicle). The number of TUNEL+ cells was elevated in renal artery segments from ARVD + Vehicle animals, but normalized in ARVD + Bendavia ($P = 0.81$ vs. normal), while superoxide production decreased, although not normalized. Furthermore, eNOS immunoreactivity that was down-regulated in the stenotic renal artery from ARVD + Vehicle pigs was preserved in pigs treated with Bendavia (Figure 6B).

3.5 RAEC studies

Incubation with tBHP decreased RAEC cardiolipin expression, which returned to normal levels upon co-incubation with Bendavia (Figure 7A). Incubation with tBHP decreased the viability of RAEC (RAEC + tBHP = 68.4%) compared with untreated RAEC (94.0%), while concurrent treatment with Bendavia protected against tBHP-induced cytotoxicity (RAEC + tBHP + Bendavia = 89.7%). The number of caspase-3+ cells and its expression rose in RAEC + tBHP, but normalized in RAEC + tBHP + Bendavia (Figure 7A and B, $P \leq 0.001$ vs. RAEC + tBHP). Similarly, the elevated *in situ* production of superoxide anion and nitrotyrosine expression in RAEC + tBHP declined in RAEC + tBHP + Bendavia cells (Figure 7A and B). Finally, eNOS immunoreactivity

and phosphorylated eNOS expression improved in cells co-incubated with Bendavia (Figure 7A and B).

3.6 Contralateral kidney

Cardiolipin expression and staining intensity in the contralateral kidney remained unchanged (see Supplementary material online, Figure S5A). Renal volume was similarly increased in the non-stenotic kidney of both ARVD groups compared with normal (see Supplementary material online, Table S3). GFR was comparably decreased in the contralateral kidney of ARVD + Vehicle and ARVD + Bendavia pigs, and cortical and medullary $R2^*$ values similarly elevated (see Supplementary material online, Figure S5B). Tubular injury and tubulointerstitial fibrosis in the contralateral kidney were similar among the groups (see Supplementary material online, Figure S5C and D). Finally, contralateral kidney (CLK) responses to Ach both *in vivo* (ΔRBF) and *in vitro* (renal artery rings) were similar among the groups (see Supplementary material online, Table S3 and Figure S5E).

4. Discussion

Our study demonstrates that, in ARVD, the post-stenotic kidney exhibits loss of mitochondrial inner membrane cardiolipin that contributes to kidney injury and dysfunction. Indeed, despite sustained renal artery stenosis and renovascular hypertension, mitochondrial protection and restoration of cardiolipin content decreased apoptosis and oxidative stress and attenuated microvascular loss in the post-stenotic kidney. Furthermore, this strategy normalized renal and endothelial function *in vivo* and *ex vivo*, improved renal oxygenation, and attenuated tubular damage and fibrosis. These results underscore the direct contribution of mitochondrial dysfunction to the pathogenesis of ARVD, and reveal a unique potential of mitochondrial-targeted therapies for preserving the ischaemic kidney in chronic experimental ARVD.

Atherosclerotic occlusion of the renal artery remains an important cause of chronic kidney failure in elderly patients and is frequently associated with serious cardiovascular complications.¹ Despite advances in diagnostic and interventional therapies, the underlying mechanisms and management regimens for ARVD patients remain controversial. Furthermore, the multi-factorial pathogenic mechanisms responsible

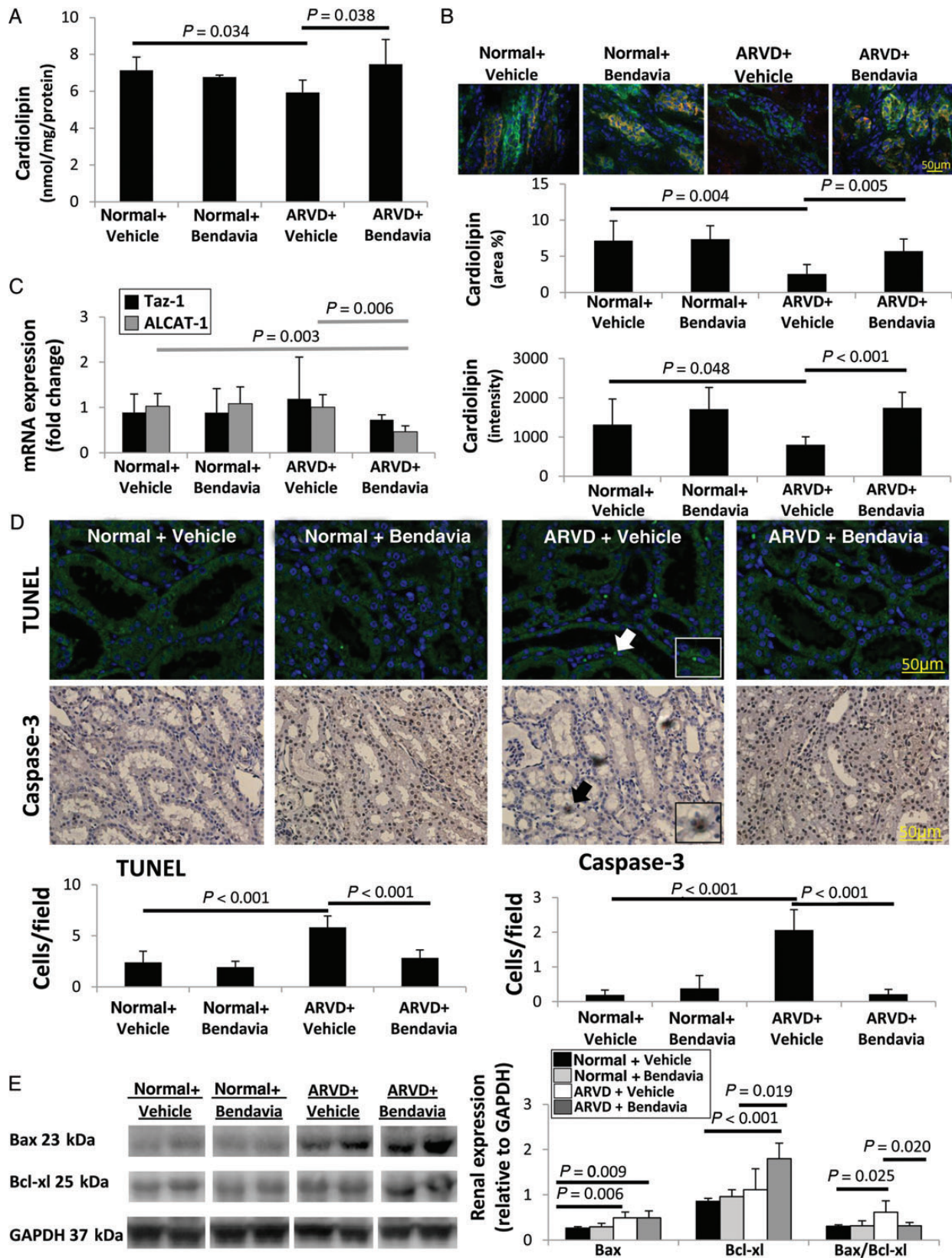


Figure 2 (A) Stenotic-kidney cardiolipin content decreased in ARVD, but was restored in ARVD + Bendavia ($n = 7$ /group). (B) Fluorescent staining for cardiolipin (red) and cytokeratin (green) confirmed decreased renal expression and staining intensity in ARVD, which was normalized in ARVD + Bendavia ($n = 7$ /group). (C) Expression of Taz-1 mRNA was unaltered, whereas ALCAT-1 was down-regulated in ARVD + Bendavia ($n = 7$ /group). (D) The numbers of TUNEL+ and caspase-3+ cells were elevated in ARVD, yet normalized in ARVD + Bendavia ($n = 7$ /group). (E) Renal protein expression and ratio of Bax and Bcl-xl ($n = 6$ /group).

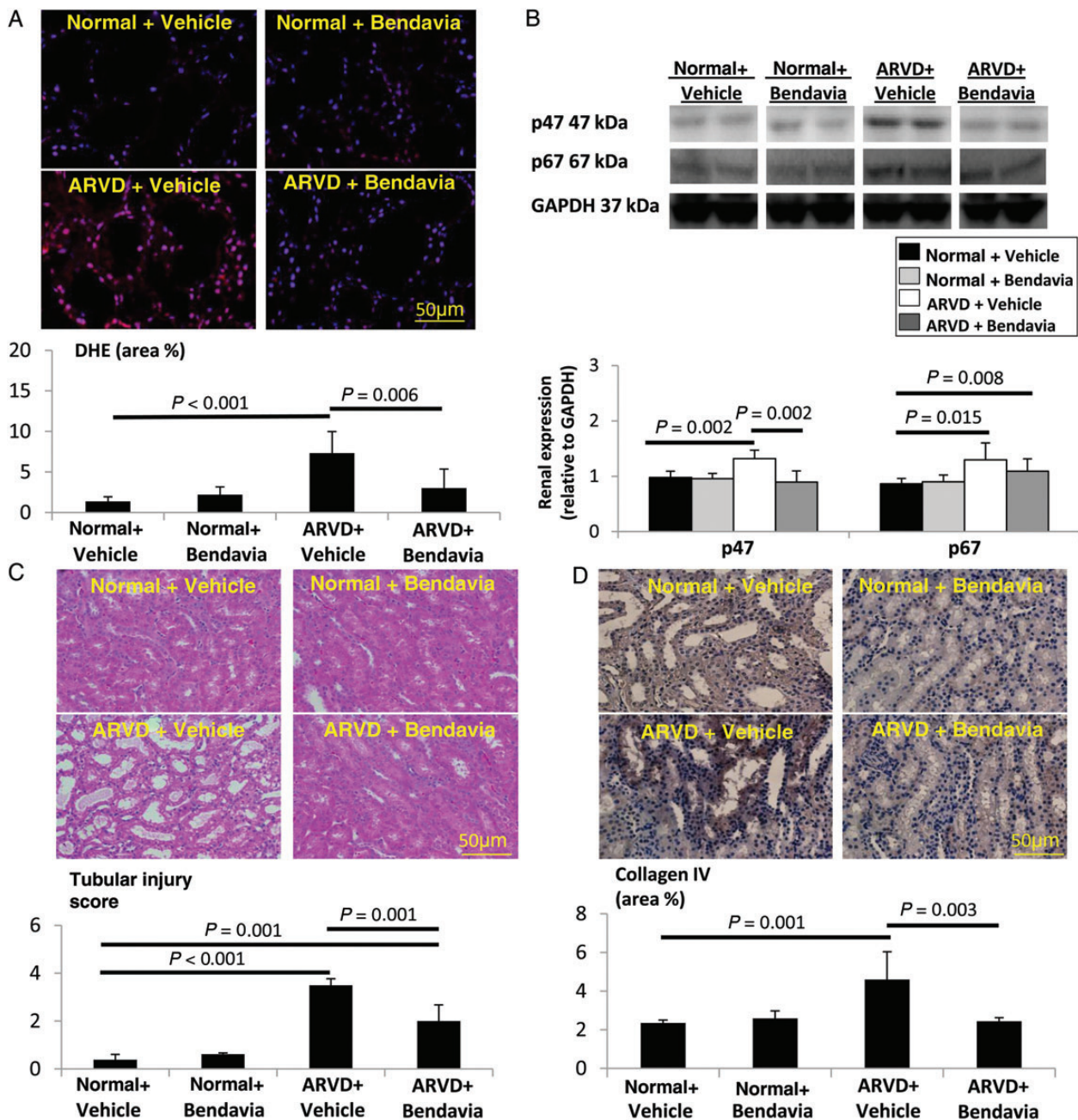


Figure 3 (A) Renal production of superoxide anion (DHE) was increased in ARVD and attenuated by Bendavia ($n = 7/\text{group}$). (B) Renal expression of p47 was restored in Bendavia-treated ARVD ($n = 6/\text{group}$). Tubular injury score (C, H&E) and collagen IV immunostaining of (D) were elevated in both ARVD groups, yet improved in ARVD + Bendavia ($n = 7/\text{group}$).

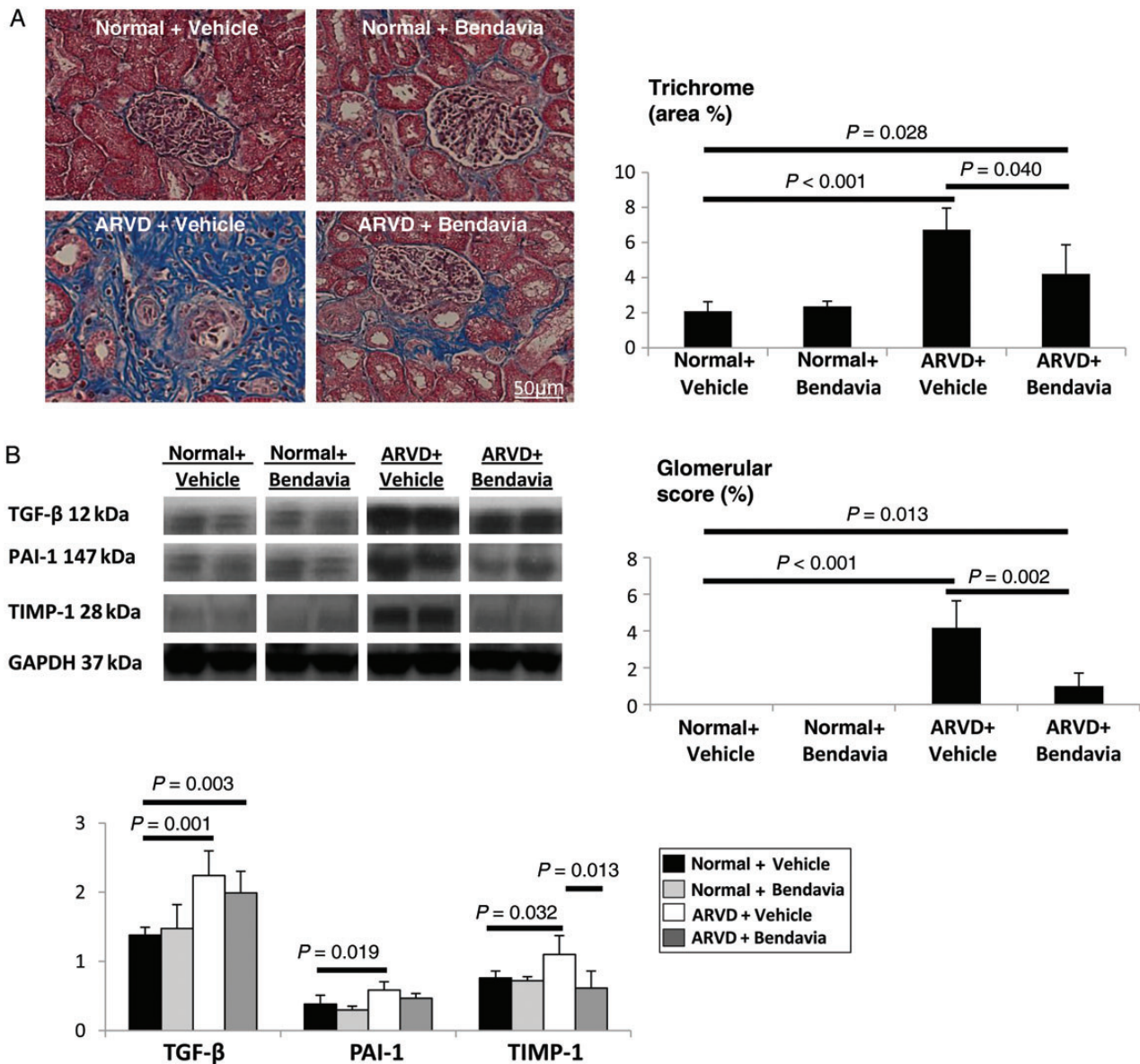
for disease progression challenge the development of effective interventions to treat these patients.²⁴

4.1 Bendavia: cellular targets and mechanisms of protection

The kidney is highly dependent on adequate function of the mitochondria that play a key role in cellular energy supply, particularly to renal tubular cells due to their transport activity.²⁵ Cardiolipin is a phospholipid uniquely located in the inner mitochondrial membrane, where it interacts with multiple mitochondrial proteins and enzymes involved in ETC assembly and function, ATP synthesis, and apoptosis.^{5–7}

Furthermore, cardiolipin modulates the stability and function of respiratory chain supercomplexes, higher-order structures that facilitate electron transfer, optimizing bioenergetic efficiency.²⁶ Therefore, strategies aimed to preserve cardiolipin might have an impact on cell function and survival.

Bendavia (MTP-131, an analogue of SS-31) is a novel cell-permeable tetrapeptide that selectively concentrates in the inner mitochondrial membrane, where it stabilizes cardiolipin and prevents its peroxidation.^{11,27} This manoeuvre sustains mitochondrial bioenergetics, and attenuates apoptosis and oxidative stress in numerous models of cardiovascular disease and acute kidney injury.^{12,13} We have recently shown



that infusion of Bendavia during revascularization of the stenotic renal artery in swine ARVD reduced acute kidney injury and subsequent microvascular rarefaction and renal remodelling, thereby improving revascularization outcomes.¹⁷ The current study extends our previous observations by revealing the capacity of mitoprotection to attenuate chronic renal injury and dysfunction in non-revascularized ARVD pigs.

Mitochondrial protection in our model is illustrated by normalization of cardiolipin content. Cardiolipin synthesized in the mitochondria undergoes continuous remodelling, governed by taz-1 and ALCAT-1 in the inner and outer mitochondrial membranes, respectively. Taz-1, an enzyme that mediates the late steps in the cardiolipin biosynthesis pathway, maintains optimal cardiolipin content and acyl-chain composition.²⁸ In contrast, ALCAT-1 is a major regulator of abnormal cardiolipin remodelling, leading to oxidative stress and mitochondrial dysfunction.²⁹ This study demonstrates that despite unchanged mRNA

expression of taz-1, Bendavia decreased mRNA expression of ALCAT-1, suggesting that Bendavia attenuates primarily pathological remodelling of cardiolipin.

Cardiolipin regulates apoptotic cell death by interacting with proteins involved in the permeabilization of the mitochondrial membranes. In addition to supporting the recruitment, oligomerization, and processing of caspase-8, cardiolipin binds Bid and t-Bid, inducing Bax activation and the subsequent outer mitochondrial membrane permeabilization.³⁰ Under normal conditions, cardiolipin interacts with cytochrome-c in the inner mitochondrial membrane, regulating its peroxidase capabilities. Oxidative damage of cardiolipin sensitizes mitochondria to calcium inducing the formation of the mPTP and the release of cytochrome-c to the cytosol. In the current study, Bendavia-induced restoration of cardiolipin decreased apoptosis, disclosed by the decreased number of TUNEL- and caspase-3-positive

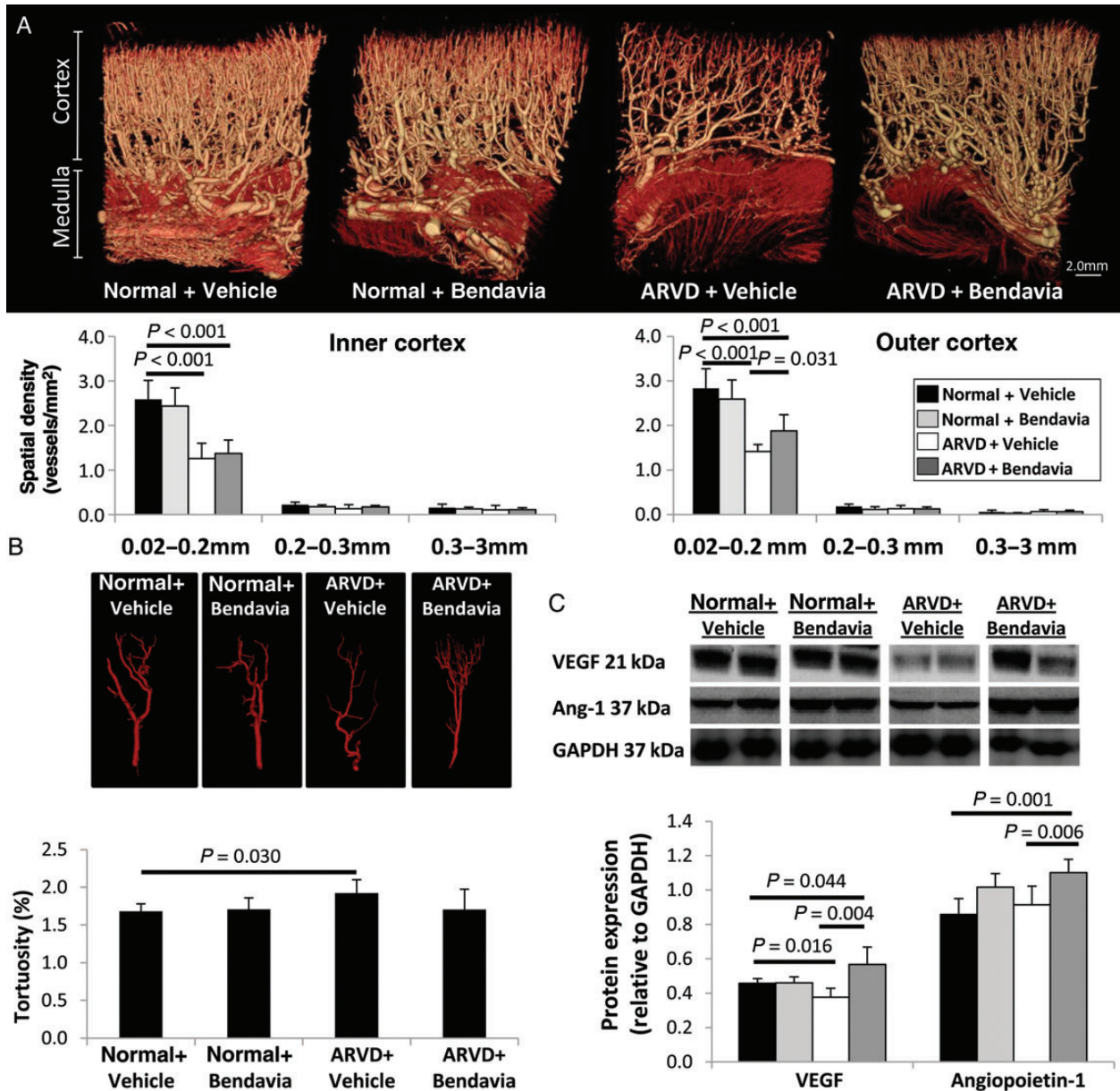


Figure 5 (A) Representative 3D micro-computed tomography images of the pig kidney and quantification of spatial density of size-specific microvessels in the inner and outer cortex ($n = 7$ /group). (B) Tomographically isolated vessels and quantification of their tortuosity ($n = 7$ /group). (C) Renal protein expression of VEGF and angiopoietin-1 was up-regulated in ARVD + Bendavia pigs ($n = 6$ /group).

cells and Bax/Bcl-xl, possibly by preventing mPTP opening and release of cytochrome-c.

Mitochondria are major sites of superoxide production, which is catalysed primarily by NAD(P)H oxidase, a multi-subunit enzyme system that transfers electrons from NADPH and couples them to molecular oxygen.³¹ Both the p47 and p67 subunits, located in the cytosol, are required to activate the membrane-bound NAD(P)H oxidase. Bendavia decreases oxidative stress and renal damage in rats with unilateral ureteral obstruction¹⁵ or with contrast media-induced acute kidney injury.³² This study corroborates these findings by showing that mitochondrial protection blunted renal oxidative stress, reflected by normalized production of superoxide anion. Interestingly, Bendavia normalized p47 (albeit not p67) expression, implicating it in modulating the assembly

of NADPH oxidase regulatory subunits. Notably, circulating levels of isoprostanes remained elevated, possibly secondary to sustained hypercholesterolaemia, arguing against major contribution of mitochondrial dysfunction to systemic oxidative stress under these conditions.

Our group has previously demonstrated that increased oxidative stress in the swine stenotic kidney is associated with downregulated VEGF expression, cortical microvascular loss, and fibrosis.⁴ Chade and Kelsen have shown that infusion of VEGF into the stenotic kidney of non-atherosclerotic RVD pigs improved renal function by stimulating microvascular proliferation and repair.^{33,34} In the current study, mitochondrial protection slightly improved microvascular spatial density and angiogenic activity (VEGF), implying improvement in the renal microvasculature. Furthermore, Bendavia improved vessel maturity, disclosed by

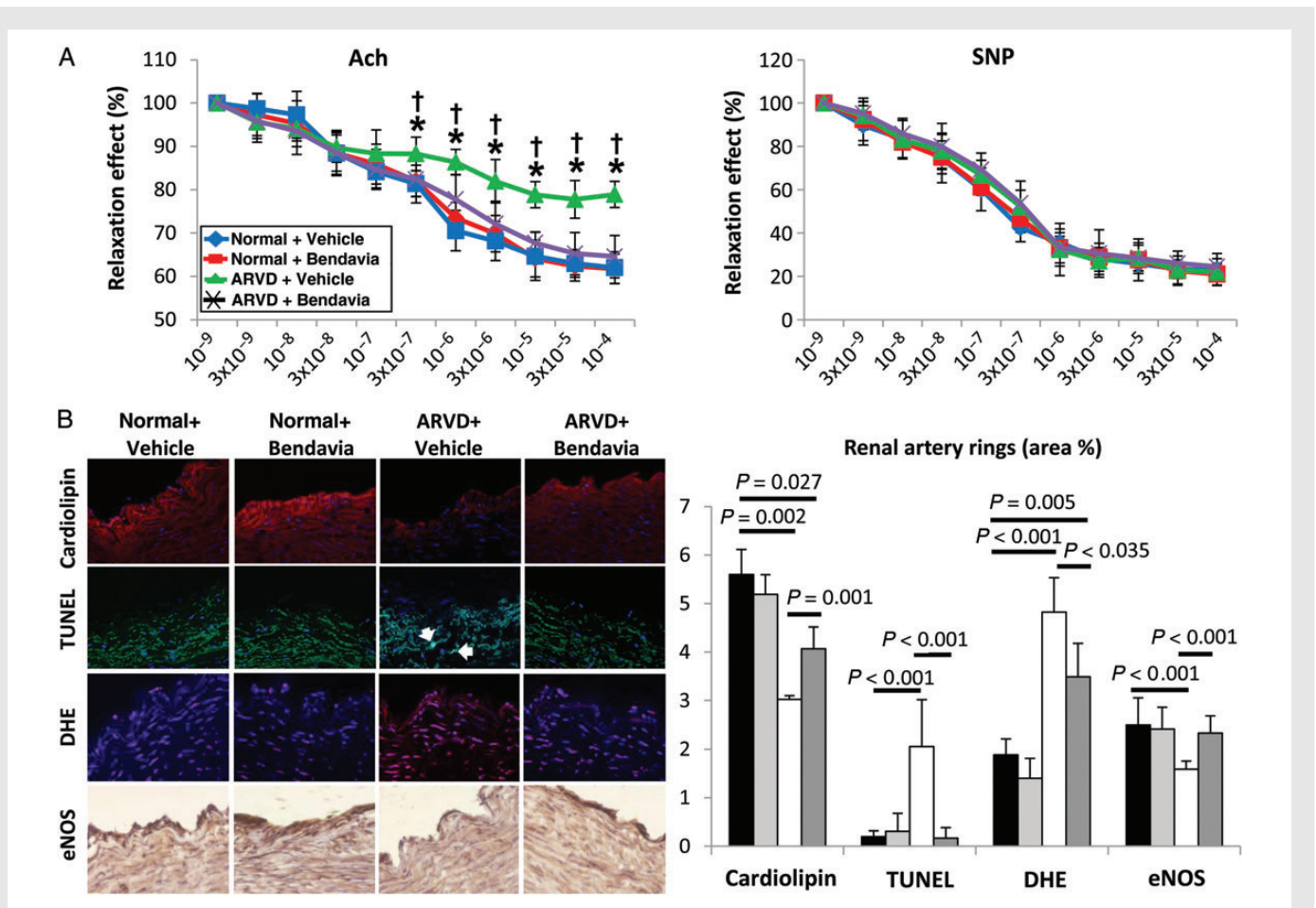


Figure 6 (A) Endothelial-dependent (left) and independent (right) relaxation responses of renal arterial segments from normal and ARVD pigs (chronically treated with Bendavia or Vehicle) to Ach and SNP ($n = 7/\text{group}$). (B) Quantification of cardiolipin expression (10N-nonyl acridine orange), apoptosis (TUNEL), DHE ($n = 7/\text{group}$), and eNOS immunoreactivity ($n = 6/\text{group}$) in stenotic-kidney artery sections. * $P \leq 0.05$ vs. Normal + Vehicle, † $P \leq 0.05$ vs. ARVD + Bendavia.

decreased tortuosity, and up-regulated renal expression of angiotensin-1. Angiotensin-1 acts in concert with VEGF to boost neovascularization, by promoting the formation of mature and functional microvessels.³⁵ Importantly, spatial density of microvessels in the outer cortex correlates directly with single-kidney GFR, suggesting that microvascular remodelling in this region is a critical determinant of renal dysfunction in ARVD.²⁰ Furthermore, Bendavia decreases renal fibrosis by normalizing collagen IV deposition, and the expression of PAI-1 and TIMP-1, major contributors to renal disease progression in ARVD.²⁴ Remarkably, mitoprotection also normalized cortical and medullary oxygenation, possibly secondary to improved microvascular density and endothelial function and thereby the integrity of the renal tubules. Renal hypoxia leads to fibrosis and capillary rarefaction, creating a vicious cycle that reduces oxygen delivery.¹⁹ These data are consistent with previous studies showing that Bendavia reduces cardiac microvascular injury associated with the no-reflow phenomenon,¹³ as well as renal tubulointerstitial injury and fibrosis, uncovering its potential to attenuate downstream scarring.^{15,32}

Renal volume, perfusion, RBF, GFR, and serum creatinine were also all normalized in ARVD + Bendavia compared to ARVD + Vehicle, despite similar blood pressure. The lack of effect on hypertension in ARVD + Bendavia suggests the recruitment of additional pressor

mechanisms,³⁶ like systemic oxidative stress (circulating isoprostanes) that remained elevated, possibly secondary to sustained systemic hypercholesterolaemia. In addition, the unchanged degree of stenosis (triggering a fall in perfusion pressure) might have activated the local renin-angiotensin system. Contrarily, ameliorated intra-renal apoptosis, oxidative stress, and fibrosis, which promote kidney disease,²⁴ might have improved function in the ARVD kidney.²⁴ Additionally, microvascular proliferation might have attenuated renal vascular resistance distal to the stenosis, improving RBF and GFR. Moreover, preserved stenotic-kidney RBF responses to Ach indicated improved renal microvascular endothelial function, confirmed *ex vivo* in macrovascular segments. Improved endothelial function may be attributed to augmented availability of nitric oxide (normalized eNOS immunoreactivity) in ARVD + Bendavia, possibly secondary to mitoprotection that reduced apoptosis and oxidative stress, denoted by up-regulated cardiolipin expression.

Indeed, studies in endothelial cells incubated with tBHP (that causes lipid peroxidation and mitochondrial dysfunction²²) confirmed that restoration of cardiolipin content decreased apoptosis and oxidative stress. Finally, cells treated with Bendavia showed increased expression of eNOS, supporting a direct effect of mitochondrial protection to improve bioavailability of nitric oxide.

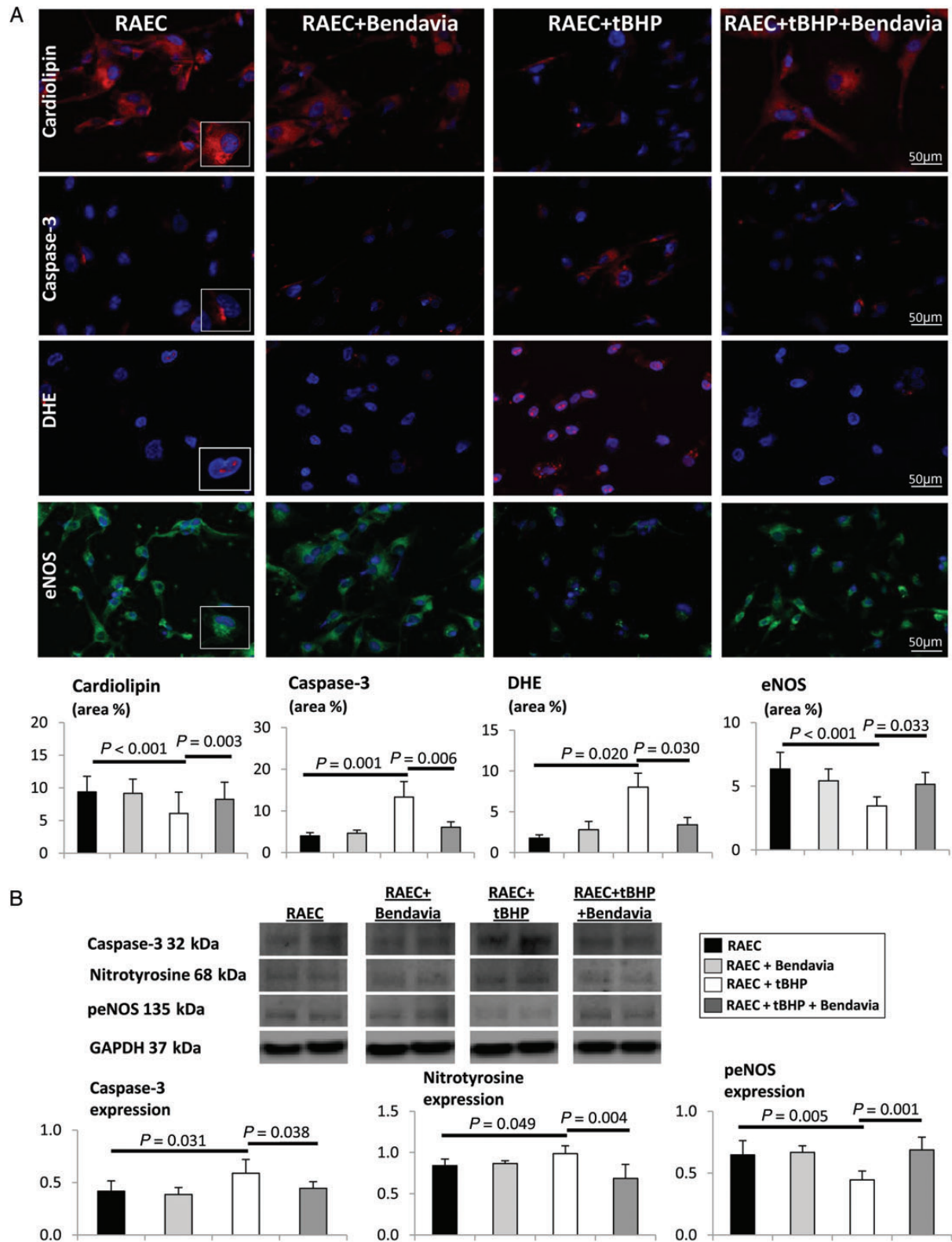


Figure 7 (A) Cardioliipin expression decreased in RAECs isolated from a normal animal and treated with tBHP, but was preserved in cells co-incubated with Bendavia, and the number of caspase-3-positive cells decreased DHE staining and eNOS immunoreactivity was normalized. (B) Expression of caspase-3, nitrotyrosine, and phosphorylated eNOS (peNOS) in untreated RAEC, RAEC + Bendavia, RAEC + tBHP, and RAEC + tBHP + Bendavia normalized by glyceraldehyde 3-phosphate dehydrogenase (GAPDH).

4.2 ARVD model: advantages and limitations

These experiments were performed in a swine model of ARVD that our group developed and characterized. The short duration of the disease, young age of the animals, and lack of additional comorbid conditions limit the applicability of this model, yet renal structural alterations resemble those observed in humans. We have shown that similar to observations in humans, atherosclerosis synergistically accelerates renal functional compromise, intra-renal inflammation, and fibrosis in the stenotic kidney.^{37–39} Furthermore, novel physiological imaging techniques that allow studying the single-kidney function and structure provided a unique opportunity to identify and assess the potential effects of Bendavia for improving renal function, reducing apoptosis and the progression to fibrosis in the ARVD kidney. Owing to a moderate elevation in blood pressure, CLK injury in our model is relatively modest, yet its oxygenation and GFR are blunted. These were not fully corrected by Bendavia, possibly because of continued hypertensive and dyslipidaemic injury, as well as relentlessly elevated levels of prostaglandin-F₂α-isoprostanes. In contrast to the stenotic kidney, cardiolipin expression in the CLK was unaltered, suggesting that in chronic ARVD mitochondrial injury (at least cardiolipin remodelling) does not play a central role in CLK injury, on which indeed Bendavia had little effect.

Interestingly, the decrease in cardiolipin staining observed in ARVD appears more dramatic than that in cardiolipin mass measured by mass spectrometry, possibly because of effects of mitochondrial membrane potential and respiration rate on the nonyl acridine orange signal.⁴⁰ Despite modest effect on microvascular density, vessel maturity was normalized in ARVD + Bendavia pigs, which might have preserved microvascular function and attenuated renal dysfunction distal to the stenosis. Hypercholesterolaemia alone that triggers mitochondrial damage and dysfunction⁴¹ might be an important modifier in our model, and the potential of Bendavia to ameliorate renal injury in hypercholesterolaemic or non-atherosclerotic RVD pigs needs further investigation. Nevertheless, the relatively minor effect of Bendavia on the CLK, which was exposed to similar levels of hypercholesterolaemia, suggests that its interaction with renal ischaemia specifically provoked mitochondrial damage. Future studies are needed to explore the effects of Bendavia on components of the renin–angiotensin system and to establish its renoprotective properties in human renovascular disease.

5. Conclusions

The post-stenotic kidney in ARVD is characterized by loss of mitochondrial cardiolipin content and composition. Mitochondrial protection improved porcine stenotic kidney haemodynamics and function, and normalized vascular endothelial function *in vivo* and *ex vivo*, implying a pivotal detrimental role of mitochondrial damage in ARVD. Mitoprotection achieved by restoring cardiolipin attenuated microvascular loss, oxidative stress, and fibrosis, uncovering a unique therapeutic potential for mitochondrial protection in restoring renal function in chronic experimental ARVD.

Supplementary material

Supplementary material is available at *Cardiovascular Research* online.

Conflict of interest: A.L. and L.O.L. serve on the Advisory Board of Stealth Peptides, Inc.

Funding

This work was supported by a grant from Stealth Peptides, Inc., and by the NIH grants (DK73608, HL77131, UL1TR000135, HL121561, DK100081, and RR018898).

References

- Conlon PJ, Little MA, Pieper K, Mark DB. Severity of renal vascular disease predicts mortality in patients undergoing coronary angiography. *Kidney Int* 2001;**60**:1490–1497.
- Cooper CJ, Murphy TP, Cutlip DE, Jamerson K, Henrich W, Reid DM, Cohen DJ, Matsumoto AH, Steffes M, Jaff MR, Prince MR, Lewis EF, Tuttle KR, Shapiro JL, Rundback JH, Massaro JM, D'Agostino RB Sr, Dworkin LD. Stenting and medical therapy for atherosclerotic renal-artery stenosis. *N Engl J Med* 2013;**370**:13–22.
- Kluge MA, Fetterman JL, Vita JA. Mitochondria and endothelial function. *Circ Res* 2013;**112**:1171–1188.
- Zhu XY, Chade AR, Rodriguez-Porcel M, Bentley MD, Ritman EL, Lerman A, Lerman LO. Cortical microvascular remodeling in the stenotic kidney: role of increased oxidative stress. *Arterioscler Thromb Vasc Biol* 2004;**24**:1854–1859.
- Klingenberg M. Cardiolipin and mitochondrial carriers. *Biochim Biophys Acta* 2009;**1788**:2048–2058.
- van Gestel RA, Rijken PJ, Surinova S, O'Flaherty M, Heck AJ, Killian JA, de Kroon AI, Slijper M. The influence of the acyl chain composition of cardiolipin on the stability of mitochondrial complexes; an unexpected effect of cardiolipin in alpha-ketoglutarate dehydrogenase and prohibitin complexes. *J Proteomics* 2010;**73**:806–814.
- Schug ZT, Gottlieb E. Cardiolipin acts as a mitochondrial signalling platform to launch apoptosis. *Biochim Biophys Acta* 2009;**1788**:2022–2031.
- Petrosillo G, Moro N, Ruggiero FM, Paradies G. Melatonin inhibits cardiolipin peroxidation in mitochondria and prevents the mitochondrial permeability transition and cytochrome c release. *Free Radic Biol Med* 2009;**47**:969–974.
- Shidoji Y, Hayashi K, Komura S, Ohishi N, Yagi K. Loss of molecular interaction between cytochrome c and cardiolipin due to lipid peroxidation. *Biochem Biophys Res Commun* 1999;**264**:343–347.
- Petrosillo G, Ruggiero FM, Paradies G. Role of reactive oxygen species and cardiolipin in the release of cytochrome c from mitochondria. *FASEB J* 2003;**17**:2202–2208.
- Birk AV, Liu S, Soong Y, Mills W, Singh P, Warren JD, Seshan SV, Pardee JD, Szeto HH. The mitochondrial-targeted compound SS-31 re-energizes ischemic mitochondria by interacting with cardiolipin. *J Am Soc Nephrol* 2013;**24**:1250–1261.
- Dai DF, Chen T, Szeto H, Nieves-Cintrón M, Kutayavin V, Santana LF, Rabinovitch PS. Mitochondrial targeted antioxidant peptide ameliorates hypertensive cardiomyopathy. *J Am Coll Cardiol* 2011;**58**:73–82.
- Kloner RA, Hale SL, Dai W, Gorman RC, Shuto T, Koomalsingh KJ, Gorman JH III, Sloan RC, Frasier CR, Watson CA, Bostian PA, Kypson AP, Brown DA. Reduction of ischemia/reperfusion injury with Bendavia, a mitochondria-targeting cytoprotective peptide. *J Am Heart Assoc* 2012;**1**:e001644.
- Sloan RC, Moukdar F, Frasier CR, Patel HD, Bostian PA, Lust RM, Brown DA. Mitochondrial permeability transition in the diabetic heart: contributions of thiol redox state and mitochondrial calcium to augmented reperfusion injury. *J Mol Cell Cardiol* 2012;**52**:1009–1018.
- Mizuguchi Y, Chen J, Seshan SV, Poppas DP, Szeto HH, Felsen D. A novel cell-permeable antioxidant peptide decreases renal tubular apoptosis and damage in unilateral ureteral obstruction. *Am J Physiol Renal Physiol* 2008;**295**:F1545–F1553.
- Szeto HH, Liu S, Soong Y, Wu D, Darrah SF, Cheng FY, Zhao Z, Ganger M, Tow CY, Seshan SV. Mitochondria-targeted peptide accelerates ATP recovery and reduces ischemic kidney injury. *J Am Soc Nephrol* 2011;**22**:1041–1052.
- Eirin A, Li Z, Zhang X, Krier JD, Woollard JR, Zhu XY, Tang H, Herrmann SM, Lerman A, Textor SC, Lerman LO. A mitochondrial permeability transition pore inhibitor improves renal outcomes after revascularization in experimental atherosclerotic renal artery stenosis. *Hypertension* 2012;**60**:1242–1249.
- Daghini E, Primak AN, Chade AR, Krier JD, Zhu XY, Ritman EL, McCollough CH, Lerman LO. Assessment of renal hemodynamics and function in pigs with 64-section multidetector CT: comparison with electron-beam CT. *Radiology* 2007;**243**:405–412.
- Ebrahimi B, Li Z, Eirin A, Zhu XY, Textor SC, Lerman LO. Addition of endothelial progenitor cells to renal revascularization restores medullary tubular oxygen consumption in swine renal artery stenosis. *Am J Physiol Renal Physiol* 2012;**302**:F1478–F1485.
- Eirin A, Zhu XY, Urbieta-Caceres VH, Grande JP, Lerman A, Textor SC, Lerman LO. Persistent kidney dysfunction in swine renal artery stenosis correlates with outer cortical microvascular remodeling. *Am J Physiol Renal Physiol* 2011;**300**:F1394–F1401.
- Eirin A, Zhu XY, Krier JD, Tang H, Jordan KL, Grande JP, Lerman A, Textor SC, Lerman LO. Adipose tissue-derived mesenchymal stem cells improve revascularization outcomes to restore renal function in swine atherosclerotic renal artery stenosis. *Stem Cells* 2012;**30**:1030–1041.
- Zhao K, Luo G, Giannelli S, Szeto HH. Mitochondria-targeted peptide prevents mitochondrial depolarization and apoptosis induced by tert-butyl hydroperoxide in neuronal cell lines. *Biochem Pharmacol* 2005;**70**:1796–1806.
- Pipinos II, Nypaver TJ, Moshin SK, Careterro OA, Beierwaltes WH. Response to angiotensin inhibition in rats with sustained renovascular hypertension correlates with response to removing renal artery stenosis. *J Vasc Surg* 1998;**28**:167–177.

24. Eirin A, Lerman LO. Darkness at the end of the tunnel: poststenotic kidney injury. *Physiology (Bethesda)* 2013;**28**:245–253.
25. Fedorova LV, Sodhi K, Gatto-Weis C, Puri N, Hinds TD Jr, Shapiro JL, Malhotra D. Peroxisome proliferator-activated receptor delta agonist, hpp593, prevents renal necrosis under chronic ischemia. *PLoS ONE* 2013;**8**:e64436.
26. Zhang M, Mileykovskaya E, Dowhan W. Gluing the respiratory chain together. Cardiolipin is required for supercomplex formation in the inner mitochondrial membrane. *J Biol Chem* 2002;**277**:43553–43556.
27. Szeto HH. Mitochondria-targeted cytoprotective peptides for ischemia-reperfusion injury. *Antioxid Redox Signal* 2008;**10**:601–619.
28. Schlame M. Cardiolipin synthesis for the assembly of bacterial and mitochondrial membranes. *J Lipid Res* 2008;**49**:1607–1620.
29. Li J, Romestaing C, Han X, Li Y, Hao X, Wu Y, Sun C, Liu X, Jefferson LS, Xiong J, Lanoue KF, Chang Z, Lynch CJ, Wang H, Shi Y. Cardiolipin remodeling by ALCAT1 links oxidative stress and mitochondrial dysfunction to obesity. *Cell Metab* 2010;**12**:154–165.
30. Gonzalez F, Schug ZT, Houtkooper RH, MacKenzie ED, Brooks DG, Wanders RJA, Petit PX, Vaz FM, Gottlieb E. Cardiolipin provides an essential activating platform for caspase-8 on mitochondria. *J Cell Biol* 2008;**183**:681–696.
31. Babior BM. NADPH oxidase. *Curr Opin Immunol* 2004;**16**:42–47.
32. Duan S-B, Yang S-K, Zhou Q-Y, Pan P, Zhang H, Liu F, Xu X-Q. Mitochondria-targeted peptides prevent on contrast-induced acute kidney injury in the rats with hypercholesterolemia. *Ren Fail* 2013;**35**:1124–1129.
33. Chade AR, Kelsen S. Reversal of renal dysfunction by targeted administration of VEGF into the stenotic kidney: a novel potential therapeutic approach. *Am J Physiol Renal Physiol* 2012;**302**:F1342–F1350.
34. Chade AR, Kelsen S. Renal microvascular disease determines the responses to revascularization in experimental renovascular disease. *Circ Cardiovasc Interv* 2010;**3**:376–383.
35. Benest AV, Salmon AH, Wang W, Glover CP, Uney J, Harper SJ, Bates DO. VEGF and angiotensin-1 stimulate different angiogenic phenotypes that combine to enhance functional neovascularization in adult tissue. *Microcirculation* 2006;**13**:423–437.
36. Garovic VD, Textor SC. Renovascular hypertension and ischemic nephropathy. *Circulation* 2005;**112**:1362–1374.
37. Chade AR, Rodriguez-Porcel M, Grande JP, Krier JD, Lerman A, Romero JC, Napoli C, Lerman LO. Distinct renal injury in early atherosclerosis and renovascular disease. *Circulation* 2002;**106**:1165–1171.
38. Chade AR, Rodriguez-Porcel M, Grande JP, Zhu X, Sica V, Napoli C, Sawamura T, Textor SC, Lerman A, Lerman LO. Mechanisms of renal structural alterations in combined hypercholesterolemia and renal artery stenosis. *Arterioscler Thromb Vasc Biol* 2003;**23**:1295–1301.
39. Chade AR, Rodriguez-Porcel M, Herrmann J, Zhu X, Grande JP, Napoli C, Lerman A, Lerman LO. Antioxidant intervention blunts renal injury in experimental renovascular disease. *J Am Soc Nephrol* 2004;**15**:958–966.
40. Jacobson J, Duchon MR, Heales SJ. Intracellular distribution of the fluorescent dye nonyl acridine orange responds to the mitochondrial membrane potential: implications for assays of cardiolipin and mitochondrial mass. *J Neurochem* 2002;**82**:224–233.
41. Oliveira HC, Cosso RG, Alberici LC, Maciel EN, Salerno AG, Dorighello GG, Velho JA, de Faria EC, Vercesi AE. Oxidative stress in atherosclerosis-prone mouse is due to low antioxidant capacity of mitochondria. *FASEB J* 2005;**19**:278–280.